

Article

Dynamic Modelling and Simulation of a Multistage Flash Desalination System

Qiu-Yun Huang, Ai-Peng Jiang *, Han-Yu Zhang , Jian Wang, Yu-Dong Xia and Lu He

School of Automation, Hangzhou Dianzi University, Hangzhou 310018, Zhejiang, China; hqy09092020@163.com (Q.-Y.H.); zhy061077@163.com (H.-Y.Z.); wj@hdu.edu.cn (J.W.); ydxia@hdu.edu.cn (Y.-D.X.); luh_hdu@163.com (L.H.)

* Correspondence: jiangaipeng@hdu.edu.cn

Abstract: As the leading thermal desalination method, multistage flash (MSF) desalination plays an important role in obtaining freshwater. Its dynamic modeling and dynamic performance prediction are quite important for the optimal control, real-time optimal operation, maintenance, and fault diagnosis of MSF plants. In this study, a detailed mathematical model of the MSF system, based on the first principle and its treatment strategy, was established to obtain transient performance change quickly. Firstly, the whole MSF system was divided into four parts, which are brine heat exchanger, flashing stage room, mixed and split modulate, and physical parameter modulate. Secondly, based on mass, energy, and momentum conservation laws, the dynamic correlation equations were formulated and then put together for a simultaneous solution. Next, with the established model, the performance of a brine-recirculation (BR)-MSF plant with 16-stage flash chambers was simulated and compared for validation. Finally, with the validated model and the simultaneous solution method, dynamic simulation and analysis were carried out to respond to the dynamic change of feed seawater temperature, feed seawater concentration, recycle stream mass flow rate, and steam temperature. The dynamic response curves of TBT (top brine temperature), BBT (bottom brine temperature), the temperature of flashing brine at previous stages, and distillate mass flow rate at previous stages were obtained, which specifically reflect the dynamic characteristics of the system. The presented dynamic model and its treatment can provide better analysis for the real-time optimal operation and control of the MSF system to achieve lower operational cost and more stable freshwater quality.

Keywords: multistage flash; seawater desalination; dynamic response; mechanism modeling



Citation: Huang, Q.-Y.; Jiang, A.-P.; Zhang, H.-Y.; Wang, J.; Xia, Y.-D.; He, L. Dynamic Modelling and Simulation of a Multistage Flash Desalination System. *Processes* **2021**, *9*, 522. <https://doi.org/10.3390/pr9030522>

Academic Editors: Anjan K. Tula and Iqbal M. Mujtaba

Received: 13 January 2021

Accepted: 11 March 2021

Published: 13 March 2021

Publisher's Note: MDPI stays neutral with regard to jurisdictional claims in published maps and institutional affiliations.



Copyright: © 2021 by the authors. Licensee MDPI, Basel, Switzerland. This article is an open access article distributed under the terms and conditions of the Creative Commons Attribution (CC BY) license (<https://creativecommons.org/licenses/by/4.0/>).

1. Introduction

With the development of society, the shortage of freshwater resources has gotten worse, and seawater desalination is an important way to solve it [1,2]. So far, among the many seawater desalination methods, multistage flash (MSF) desalination leads the way in the desalination industry because of its high reliability, large capacity of single units, and good water quality [3–6]. With the MSF desalination process becoming more sophisticated, it is necessary to establish a dynamic model of the MSF process [7–9]. Dynamic models can be used to solve problems related to the transient behaviors of the device, such as control strategies, process interaction and troubleshooting, reliability and stability analysis, and startup and shutdown conditions. Therefore, it is of great significance to establish a strict dynamic model and simulation analysis of the system.

Since the 1970s, the dynamic modeling and analysis of MSF have been gradually carried out on the basis of steady-state research. Previously, Glueck and Bradshaw [10] studied the dynamic model of the MSF process and presented a dynamic model, including the energy difference balance between the steam space and the flash chamber distillate, but they did not provide simulation results. Ulrich [11] applied the model to simulate an MSF experimental device containing 6-stage flash chambers and gave the simulation results of the system. However, the simulation results had significant drawbacks in the disturbance

of the cooling brine flow rate. Later, Rimawi [12] established a dynamic mechanism model of a one-through (OT)-MSF desalination system and provided a simultaneous solution of the mass balance equation and the energy balance equation, observed within 15 s; however, a dynamic model of the BR-MSF system was not carried out. Husain [13] et al. not only discussed the application of MSF steady-state modeling in parameter analysis but also established dynamic models in offline and online states. On this basis, Husain [14] et al. continued to improve the model. The dynamic characteristic of distillate production was considered in the original model, and the simulations were carried out using the SPEEDUP software platform. The results were compared to the data of the actual factory, which was consistent. However, the dynamic simulation accounted for only a small proportion and drawbacks. For example, only the dynamic responses of steam temperature and flow rate to brine levels were discussed. Additionally, the SPEEDUP software could not be directly used for real-time control and operation of the industrial process.

Since the 21st century, research on the dynamic modeling and simulation of MSF devices has become more complicated. Bogle [15] et al. established the MSF dynamic model on the platform of commercial software gPROMS and solved it using the Newton iterative method. However, the heat loss of the demister and the secondary evaporation of the distillate were not considered in this model, and the solution was still not suitable for real-time operation. In addition, the flow rate was simply defined as a function of flash chamber pressure, and the influences of orifice size, the pressure drop between the two stages, and the density of steam and brine on the flow rate were not considered. Mazzotti [16] et al. established a dynamic model considering the geometric characteristics of the flash chamber and the variation of physical parameters of water, steam, and brine with temperature and concentration, but the work content of dynamic response was not rich enough. Alatiqi [17] et al. conducted experimental measurements on the dynamic response of the MSF seawater desalination system with 19-stage flash chambers and analyzed the dynamic characteristics of the system. Their work is impressive and can be used to modify the models based on the first principle since it is not easy to solve the complicated MSF model, with its many dynamic and algebraic equations, directly and to study the dynamics of the MSF process. Hala [18] et al. conducted continuous dynamic response analysis of the system under the gPROMS platform but did not carry out mechanism modeling and simulation. The authors focused on the analysis of the maximum range of variation of system-related parameters. With regard to the depth of MSF system research, Alsadaie and Mujtaba [19] established the BR-MSF dynamic model in 2016, which was optimized with the lowest operating cost. There was no dynamic response analysis in this paper. Subsequently, Alsadaie and Mujtaba [20] considered the effect of noncondensable gases and established the dynamic model of the system on the gPROMS platform; in the main, the influence of noncondensable gases on the steady-state of the system was analyzed and their work provides a good foundation for dynamic analysis and real-time operation. In the same year, Alsadaie and Mujtaba [21] carried out dynamic modeling and analysis for the heat exchanger fouling problem in the system. Furthermore, Lappalainen [22] et al. established a BR-MSF dynamic nonmechanism model and used a local phase equilibrium and simultaneous mass, momentum, and energy solver for simulation, which proposed a new solution for whole-system dynamic simulation research.

The above work by the author has essential pioneering significance for MSF dynamic simulations. However, the lack of a more sophisticated dynamic model and easily implemented treatment for real-time optimization still hamper the further research of MSF dynamic simulations. Based on the previous work, the influence of physical parameters, with the change of brine concentration and temperature, nonideal difference and heat loss of demister on the system performance, and the phenomenon of unequal temperature drop in each flash stage, is considered in this paper. At the same time, this paper also considers the compensation effect of the recycled brine flow rate on the seawater temperature and establishes a relatively complete and realistic dynamic mechanism model. Based on the verification and analysis of the model, the dynamic process of feed seawater temperature

(T_{sea}), feed seawater salt concentration (C_F), recycle stream mass flow rate (W_{Re}), and steam temperature (T_{steam}) were simulated and analyzed. For the quick and easy implementation of the dynamic simulation, the dynamic equations are discretized with the Runge–Kutta algorithm and solved with the Interior Point solver in the MATLAB platform. These lay a foundation and guarantee a further understanding of the dynamic change of system state and real-time optimal operation.

2. Modeling of the Multistage Flash (MSF) Process

2.1. Multistage Flash (MSF) Process Description

The MSF desalination system has two structures, which are the one-through multistage flash (OT-MSF) seawater desalination system and the brine-recirculation multistage flash (BR-MSF) seawater desalination system [23–26]. The brine-recirculation type of MSF process is said to be the industry standard [27], so the dynamic simulation and analysis in this article are based on the BR-MSF system; the flowsheet of the BR-MSF system is shown in Figure 1.

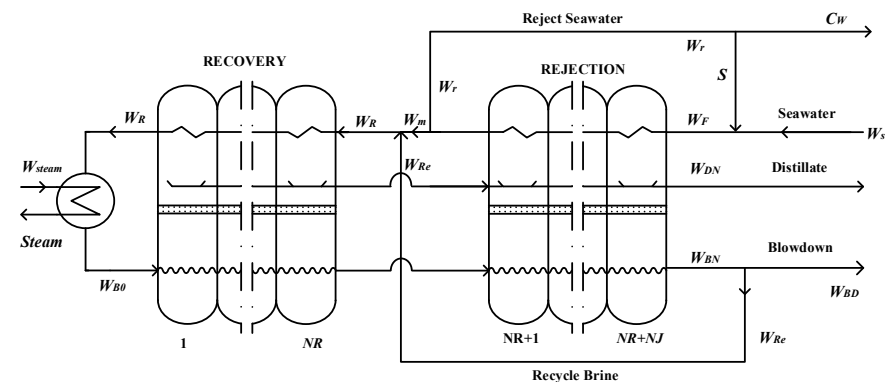


Figure 1. Multistage flash (MSF) desalination system.

The BR-MSF system is composed of a brine heater, a heat rejection section, a heat recovery section, splitters, and mixers. As shown in Figure 1, feed seawater is preheated through the condenser tube of the heat rejection section and divided into two parts; one is returned to the sea and the other is mixed with the recycled brine. The mixed brine enters the end of the heat recovery section and is heated step by step while condensing the flash steam in the flash chamber. Finally, the mixed brine flows out from the first stage of the heat recovery section, enters the brine heater for further heating, and flows into the first stage flash chamber at the highest temperature. As the pressure of the flash chamber decreases step by step, the flash stream enters the flash chamber and evaporates immediately. The generated steam passes through the condensers and drops into the distillate trays after being condensed. The process is repeated until the last stage is reached, the concentrated brine is rejected, the distillate is extracted, and a part of the brine is reused as recycled brine.

2.2. Dynamic Mathematical Modeling of the Multistage Flash (MSF) Process

The complete dynamic mathematical model of the BR-MSF desalination system includes four parts: the brine heater module, the flash chamber module, the brine heater module, the splitters and mixers module, and physical parameter equations. Next, the above four parts are modeled based on the following main assumptions:

1. The distillate from whichever stage is salt-free;
2. Noncondensable gases are ignored;
3. The system is adiabatic;
4. The influence of the pump is not considered;
5. The evaporation of freshwater is ignored;
6. The amount of flashing seawater in the condenser tubes remains constant, and there is no accumulation of salt.

2.2.1. Model of Brine Heater Module

The brine heater is one of the main pieces of equipment of the BR-MSF system; its structure is shown in Figure 2.

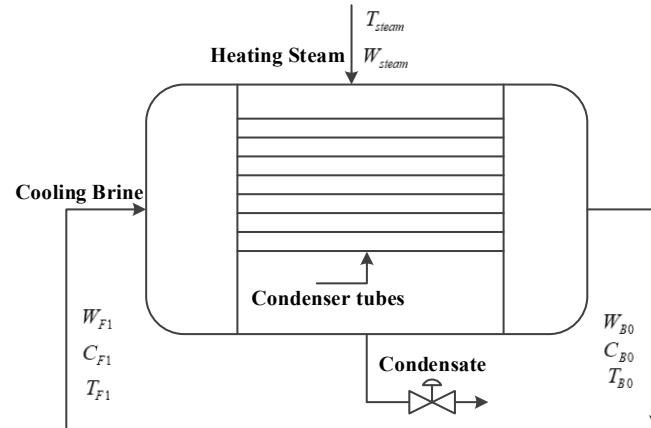


Figure 2. Structure chart of the brine heater.

The heating steam enters the brine heater at a certain temperature and flow rate, flows through the condenser tubes, and is finally pumped away by the condensing pump. During this period, the cooling brine in the condenser tubes is heated to the top brine temperature (TBT) and enters the first flash chamber for flash. Then, the above process is transformed into a mathematical model, in which the brine heater is generally regarded as the 0-th flash chamber.

Mass balance:

$$W_{B0} = W_{F1} \quad (1)$$

Salt mass balance:

$$C_{B0} = C_{F1} \quad (2)$$

where W_{B0} is the flashing brine mass flow rate leaving the brine heater, in $\text{kg}\cdot\text{h}^{-1}$; W_{F1} is the flashing seawater mass flow rate leaving Stage 1, in $\text{kg}\cdot\text{h}^{-1}$; C_{B0} is the salt concentration in the flashing seawater leaving the brine heater, in wt %; C_{F1} is the salt concentration of flashing seawater leaving Stage 1, in wt %.

Assuming that the amount of brine holdup in the condenser tubes remains unchanged and there is no salt accumulation in the condenser tubes, then:

$$\frac{d}{dt} M_{B0} = 0 \quad (3)$$

$$\frac{d}{dt} (M_{B0} C_{F0}) = 0 \quad (4)$$

where M_{B0} refers to the brine holdup in the brine heater, in kg; C_{F0} is the salt concentration of flashing seawater leaving the brine heater, in wt %.

Heating steam enthalpy balance:

$$W_{steam} \lambda_{steam} = U_H A_H \frac{T_{B0} - T_{F1}}{\ln \frac{T_{steam} - T_{F1}}{T_{steam} - T_{B0}}} \quad (5)$$

Overall enthalpy balance:

$$M_{B0} \frac{dh_{B0}}{dt} = W_{F1} (h_{B0} - h_{F1}) - U_H A_H \frac{T_{B0} - T_{F1}}{\ln \frac{T_{steam} - T_{F1}}{T_{steam} - T_{B0}}} \quad (6)$$

where W_{steam} is the steam mass flow rate, in $\text{kg}\cdot\text{h}^{-1}$; U_H is the overall heat transfer coefficient at the brine heater, in $\text{kcal}\cdot(\text{m}^2\cdot\text{h}\cdot^\circ\text{C})^{-1}$; A_H is the heat transfer area of the brine heater, in m^2 ; T_{B0} is the temperature of flashing brine leaving the brine heater, in $^\circ\text{C}$; T_{F1} is the temperature of cooling brine leaving Stage j , in $^\circ\text{C}$; λ_{steam} is the latent heat of the steam, in $\text{kcal}\cdot\text{kg}^{-1}$; h_{B0} is the specific enthalpy of the brine heater, in $\text{kcal}\cdot\text{kg}^{-1}$; h_{F1} is the specific enthalpy of flashing seawater at Stage j , in $\text{kcal}\cdot\text{kg}^{-1}$. λ_{steam} , h_{B0} , and h_{F1} in the above model are functions of concentration and temperature. For specific formulas, please refer to the physical parameter equations.

2.2.2. Model of the Flash Chamber Module

As shown in Figure 3, the j -th stage flash chamber can be divided into four parts: the brine pool, the vapor space, the product tray, and condenser tubes. At the same time, each stage of the flash chamber includes three steps: stream flash, steam condensation, and seawater preheating. Then, based on the four major components and three basic links, dynamic modeling of the flash chamber is carried out. In the process of modeling, thermodynamic loss, the variation of physical parameters with temperature and concentration, the difference of nonideality, and the basic physicochemical phenomenon of an unequal temperature difference between different stages were considered. Considering that there is very little evaporation of freshwater in the distillate tray, the evaporation of freshwater is ignored in this model. The flash chamber module equations in this paper refer to the research of Mazzotti et al. [16].

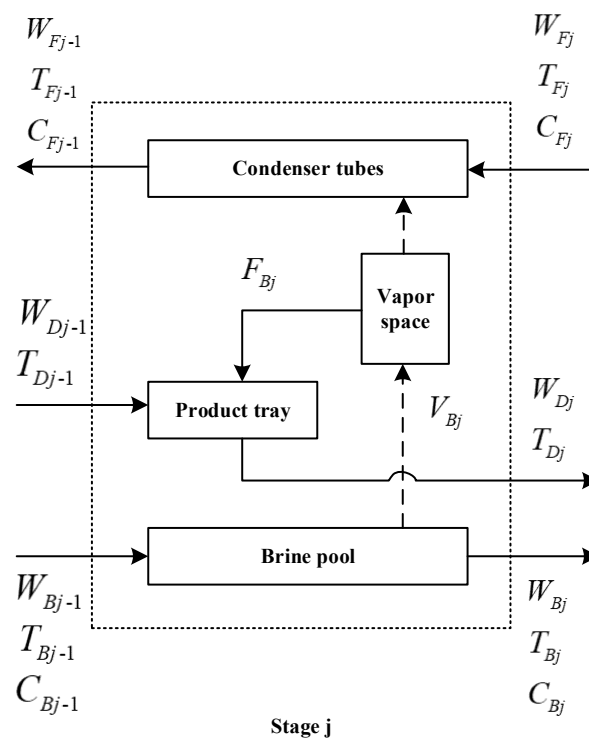


Figure 3. Structure chart of the j -th stage flash chamber.

Flashing brine mass balance:

$$\frac{d}{dt}M_{Bj} = W_{Bj-1} - W_{Bj} - V_{Bj} \quad (7)$$

where $M_{Bj} = \rho_{Bj} * V$ represents the flashing brine holdup in the j -th stage flash chamber, in kg ; V is the volume of flashing brine holdup, in m^3 ; W_{Bj} is the flashing brine mass flow rate leaving Stage j , in $\text{kg}\cdot\text{h}^{-1}$; V_{Bj} is the evaporation capacity of brine at Stage j , in $\text{kg}\cdot\text{h}^{-1}$.

Flashing brine salt balance:

$$M_{Bj} \frac{d}{dt} C_{Bj} = W_{Bj-1} C_{Bj-1} - C_{Bj} (W_{Bj-1} - V_{Bj}) \quad (8)$$

where C_{Bj} is the salt concentration in the flashing brine leaving stage j , in wt %.

Flashing brine energy balance:

$$M_{Bj} \cdot CP_{Bj} \frac{d}{dt} T_{Bj} = W_{Bj-1} (h_{Bj-1} - h_{Bj}) - V_{Bj} (h_{VBj} - h_{Bj}) \quad (9)$$

where CP_{Bj} is the heat capacity of brine leaving Stage j , in $\text{kcal} \cdot (\text{kg} \cdot ^\circ\text{C})^{-1}$; T_{Bj} is the temperature of flashing brine leaving Stage j , in $^\circ\text{C}$; h_{Bj} is the specific enthalpy of flashing brine at Stage j , $\text{kcal} \cdot \text{kg}^{-1}$.

Distillate mass balance:

$$\frac{dM_{Dj}}{dt} = W_{Dj-1} - W_{Dj} + F_{Dj} \quad (10)$$

where $M_{Dj} = \rho_{Dj} * V$ represents the distillate holdup in the j -th stage flash chamber, in kg; V is the volume of distillate holdup, in m^3 ; W_{Dj} is the distillate mass flow rate leaving Stage j , in $\text{kg} \cdot \text{h}^{-1}$; F_{Dj} is the steam condensation at Stage j , in $\text{kg} \cdot \text{h}^{-1}$.

Distillate energy balance:

$$\frac{d(M_{Dj} h_{Dj})}{dt} = W_{Dj-1} h_{Dj-1} - W_{Dj} h_{Dj} + F_{Dj} h_{FDj} \quad (11)$$

where h_{Dj} is the specific enthalpy of distillate at Stage j , $\text{kcal} \cdot \text{kg}^{-1}$; h_{FDj} is the specific enthalpy of condensation at Stage j , in $\text{kcal} \cdot \text{kg}^{-1}$.

Temperature relationship between distillate and flashing brine:

$$T_{Bj} = T_{Dj} + \Delta BPE_j + \Delta NETD_j + \Delta TL_j \quad (12)$$

where BPE represents boiling point elevation, $NETD$ represents the nonequilibrium allowance, and TL represents the temperature loss due to demister and condenser; the specific calculation formula is shown in the physical parameter equations; T_{Dj} is the temperature of distillate leaving Stage j , in $^\circ\text{C}$.

Steam mass balance:

$$\frac{dM_{Vj}}{dt} = V_{Bj} - F_{Dj} \quad (13)$$

where $M_{Vj} = \rho_{Vj} * V$ represents the steam holdup in the j -th stage flash chamber, in kg, and V is the volume of steam holdup, in m^3 .

Steam energy balance:

$$M_{Vj} CP_{Vj} \frac{dT_{Vj}}{dt} = F_{Dj} (h_{VBj} - h_{FDj}) - U_j A \frac{T_{Fj} - T_{Fj+1}}{\ln \frac{T_{Dj} - T_{Fj+1}}{T_{Dj} - T_{Fj}}} \quad (14)$$

where CP_{Vj} is the heat capacity of the flashing steam leaving Stage j , in $\text{kcal} \cdot (\text{kg} \cdot ^\circ\text{C})^{-1}$; T_{Vj} is the temperature of flashed vapor at Stage j , in $^\circ\text{C}$; h_{VBj} is the specific enthalpy of steam at Stage j , $\text{kcal} \cdot \text{kg}^{-1}$; h_{FDj} is the specific enthalpy of condensation at Stage j , $\text{kcal} \cdot \text{kg}^{-1}$; U_j is the overall heat transfer coefficient at Stage j , in $\text{kcal} \cdot (\text{m}^2 \cdot \text{h} \cdot ^\circ\text{C})^{-1}$; T_{Fj} is the temperature of cooling brine leaving Stage j , in $^\circ\text{C}$.

Temperature relationship between distillate and steam:

$$T_{Vj} = T_{Dj} + \Delta TL_j \quad (15)$$

where ΔTL_j is the temperature difference loss, in $^\circ\text{C}$.

Assuming that the amount of flashing seawater in the condenser tubes remains constant and there is no accumulation of salt, the conservation equations of flashing seawater mass and salt in the condenser tubes are as follows:

$$\frac{dM_{Fj}}{dt} = 0 \quad (16)$$

$$\frac{d(M_{Fj}C_{Fj})}{dt} = 0 \quad (17)$$

where M_{Fj} represents the flashing seawater holdup in the j -th stage flash chamber, in kg; C_{Fj} is the salt concentration of flashing seawater leaving Stage j , in wt %. Because of the constraint of the condenser tubes, its value remains constant during the flashing process, which can be obtained from the product of the volume of the condenser tubes and the density of the flashing brine.

Condenser tubes energy balance:

$$M_{Vj}CP_{Vj} \frac{dT_{Vj}}{dt} = F_{Dj}(h_{VBj} - h_{FDj}) - U_j A \frac{T_{Fj} - T_{Fj+1}}{\ln \frac{T_{Dj} - T_{Fj+1}}{T_{Dj} - T_{Fj}}} \quad (18)$$

Volume constraint of the flash chamber:

$$V = \frac{MV_j}{\rho_{Vj}} + \frac{MB_j}{\rho_{Bj}} + \frac{MD_j}{\rho_{Dj}} + V_{TUBE} \cdot N_{TUBE} \quad (19)$$

where ρ_{Vj} is the density of steam at Stage j , $\text{kg} \cdot \text{m}^{-3}$; ρ_{Bj} is the density of flashing brine at Stage j , $\text{kg} \cdot \text{m}^{-3}$; ρ_{Dj} is the density of distillate at Stage j , $\text{kg} \cdot \text{m}^{-3}$; V_{TUBE} is the volume of the condenser tube, m^3 ; N_{TUBE} is the number of condenser tubes.

2.2.3. Model of the Splitters and Mixers Module

Splitters:

$$W_{BD} = W_{BN} - W_{Re} \quad (20)$$

$$W_m = W_F - W_r \quad (21)$$

$$S = W_r - C_w \quad (22)$$

Equations (20)–(22) express the flow relationship of the three splitters, respectively. W_{BD} is the blowdown mass flow rate, in $\text{kg} \cdot \text{h}^{-1}$. W_{BN} is the flashing brine mass flow rate leaving Stage N , in $\text{kg} \cdot \text{h}^{-1}$. W_m is the make-up brine mass flow rate, in $\text{kg} \cdot \text{h}^{-1}$. W_F is the flashing seawater mass flow rate to the rejection section, in $\text{kg} \cdot \text{h}^{-1}$. S is the reject recycled mass flow rate, in $\text{kg} \cdot \text{h}^{-1}$. W_r is the mass flow rate to the reject seawater splitter, in $\text{kg} \cdot \text{h}^{-1}$. C_w is the rejected seawater mass flow rate, in $\text{kg} \cdot \text{h}^{-1}$.

Mixers:

$$W_R = W_{Re} + W_m \quad (23)$$

$$W_R C_R = W_{Re} C_{Re} + W_m C_m \quad (24)$$

$$W_R h_R = W_{Re} h_{Re} + W_m h_m \quad (25)$$

$$W_F = S + W_S \quad (26)$$

$$W_F h_{W_F} = S h_S + W_S h_{W_S} \quad (27)$$

Equations (23) and (26) express the flow relationship of the two mixers, respectively. Equation (24) expresses the salt balance at one of the mixers. Equations (25) and (27) express the energy balance of the mixers. W_R is the cooling brine mass flow rate to the recovery section, in $\text{kg} \cdot \text{h}^{-1}$. C_R is the salt concentration in the cooling brine to the recovery section, in wt %. C_{Re} is the recycled brine concentration, in wt %. C_m is the salt concentration in make-up water, in wt %. h_R is the specific enthalpy of stream to the recovery section, in

$\text{kcal}\cdot\text{kg}^{-1}$. h_{Re} is the specific enthalpy of the recycled brine, in $\text{kcal}\cdot\text{kg}^{-1}$. h_m is the specific enthalpy of the make-up brine, in $\text{kcal}\cdot\text{kg}^{-1}$. W_F is the flashing seawater mass flow rate to the rejection section, $\text{kg}\cdot\text{h}^{-1}$. W_S is the seawater mass flow rate, in $\text{kg}\cdot\text{h}^{-1}$. h_{W_F} is the specific enthalpy of the brine at the entrance of the rejection section, in $\text{kcal}\cdot\text{kg}^{-1}$. h_S is the specific enthalpy of recycled brine at the rejection stage, in $\text{kcal}\cdot\text{kg}^{-1}$. h_{W_S} is the specific enthalpy of feed seawater, in $\text{kcal}\cdot\text{kg}^{-1}$.

2.2.4. Physical Parameter Equations

The MSF desalination system exhibits a strong nonlinearity. In order to achieve better simulation performance, the physical and chemical properties of the model variables in the system must be well characterized. The physical parameter equations in this paper refer to the research of Woldai et al. [28] and Helal et al. [29].

Specific heat capacity calculation equation:

$$CP_D = 1.001183 - 6.1666652 \times 10^{-5}T_D + 1.3999989 \times 10^{-7}T_D^2 + 1.3333336 \times 10^{-9}T_D^3 \quad (28)$$

Equation (28) is integrated between the reference temperature of 32 °F and the boiling temperature in °F to obtain the following equation:

$$CP_B = [1 - CB(0.011311 - 1.146 \times 10^{-5}T_B)] \times CP_D \quad (29)$$

Enthalpy calculation equation:

$$h_V = 596.912 + 0.46694T_S - 0.000460256T_S^2 \quad (30)$$

$$h_B = CP_B \cdot T_B \quad (31)$$

$$h_D = CP_D \cdot T_D \quad (32)$$

Calculation equation of flash temperature difference loss:

$$BPE = C \cdot T^2 / (266919.6 - 379.669T + 0.334169T^2) \times [565.757/T - 9.81559 + 1.54739 \ln T - C(337.178/T - 6.41981 + 0.922753 \ln T) + C^2(32.681/T - 0.55368 + 0.079022 \ln T)] \quad (33)$$

where $C = (19.819C_B)/(1 - C_B)$.

$$NETD = \frac{195.556 \times (H_j/0.0254)^{1.1} (\omega_j \times 0.6706 \times 10^{-3})^{0.5}}{(1.8 \times \Delta T_B + 32)^{0.25} T_S^{2.5}} \quad (34)$$

where $\omega_j = WF/w_j$; w_j represents the width of the flash chamber; H_j represents the flashing brine level in the j -th stage flash chamber; ΔT_B represents the flashing brine temperature difference between the two stages.

$$TL = \exp(1.885 - 0.02063T_D)/1.8 \quad (35)$$

Heat-transfer coefficient:

$$U = 4.8857/(y + z + 4.8857f) \quad (36)$$

$$y = [0.0013(v \times D^i)^{0.2}]/[(0.2018 + 0.0031 \times T)v] \quad (37)$$

$$z = 0.1024768 \times 10^{-2} - 0.7473939 \times 10^{-5}T_D + 0.999077 \times 10^{-7}T_D^2 - 0.430046 \times 10^{-9}T_D^3 + 0.6206744 \times 10^{-12}T_D^4 \quad (38)$$

3. Model Solution Strategy and Validation

3.1. Degree of Freedom Analysis

The degree of freedom analysis is an important step before solving the model. It is important to ensure that the model equations have a unique relationship between all inputs and outputs [30]:

$$N_f = N_v - N_e = 0 \quad (39)$$

where N_f is the degree of freedom, N_v is the number of variables, including input and output, and N_e is the number of independent differential and algebraic equations.

When $N_f = 0$, it is the best case; the system can correspond to the unique solution. When $N_f < 0$, the number of variables is greater than the number of equations, and additional model equations need to be established. When $N_f > 0$, the number of variables is less than the number of equations, and the system has not determined enough variables.

The flash chamber is divided into four parts for the degree of freedom analysis: there are 4 unknown variables in the flash chamber part, 3 unknown variables in the product tray part, and 3 unknown variables in the condenser tube part. There are 5 unknown variables in the brine heater. In summary, there are 13 unknown variables in each stage of the flash chamber, 5 unknown variables in the brine heater, and 9 unknown variables in the splitters and mixers module. If the BR-MSF device has N stages, the system has $(13N + 14)$ unknown variables.

Regardless of physical parameters such as enthalpy value, specific heat capacity, and heat loss, $N_v = N_e = (13N + 14)$ in the model. From Equation (39), $N_f = 0$. Therefore, the BR-MSF dynamic model established in this paper is complete and has a unique solution.

It is impractical to directly solve the model with so many dynamic and physical equations. Hence, the dynamic equations were firstly described into algebraic equations by the Runge–Kutta algorithm; then, all the equations, including discrete dynamic equations and physical equations, were put together by simultaneous strategy, and the discretized model, in the form of nonlinear programming, was solved by the Interior Point solver through sparsity treatment in the MATLAB platform in order to carry out the simulation quickly. To fully respond to the dynamic process with different disturbances, the entire simulation time is set as 7200 s, and the interval is set as 20 s. Therefore, the model was discretized into 360 parts in the whole-time domain. Under conventional conditions, one simulation work can be finished within 50 s under the MATLAB platform to solve the discretized model with the Interior Point solver. The platform and model solution strategy lay a foundation and guarantee for real-time optimal operation in future work.

3.2. Model Validation

As the research of Rosso et al. [31] is based on real industrial data, this paper uses the system parameters in the paper by Rosso et al. The system consists of 16-stage flash chambers ($N = NJ + NR$), 3-stage flash chambers ($NJ = 3$) in the heat discharge section, and 13-stage flash chambers ($NR = 13$) in the heat recovery section. The relevant parameters of the brine heater and the flash chamber are shown in Tables 1 and 2; the initial operation parameters in the simulation process are shown in Table 3.

Table 1. Brine heater parameters of the multistage flash (MSF) system.

Parameters	Unit	Numerical Value
Internal diameter of condenser (D_H^i)	m	0.0220
Internal diameter of condenser (D_H^0)	m	0.0244
Length of condenser (L_H)	m	12.2
Heat transfer area (A_H)	m ²	3530
Fouling factor (f_H)	(h·m ² ·K)/kcal	1.86×10^{-4}

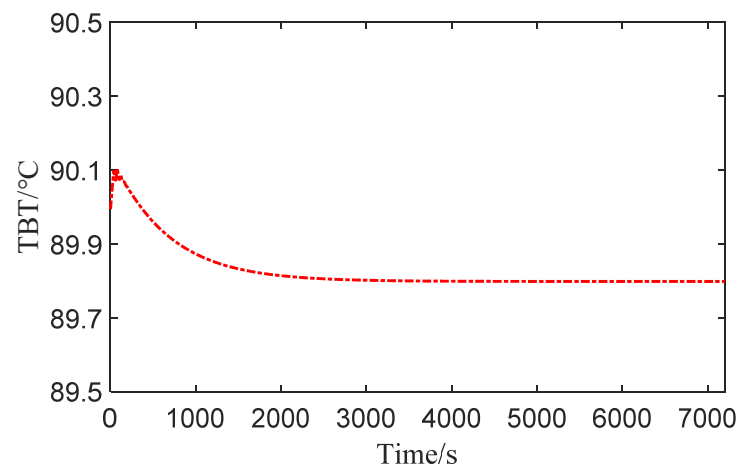
Table 2. Flash chamber parameters of the MSF system.

Parameters	Unit	Heat Recovery Section	Heat Rejection Section
Internal diameter of condenser (D_H^i)	m	0.0220	0.0239
Internal diameter of condenser (D_H^0)	m	12.2	10.7
Length of condenser (L_H)	m	3995	3530
Heat transfer area (A_H)	m ²	12.2	10.7
Fouling factor (f_H)	(h·m ² ·K)/kcal	1.4×10^{-4}	2.33×10^{-5}

Table 3. Dynamic simulation operation parameters of the MSF system.

Parameters	Unit	Numerical Value
Feed seawater mass flow rate (W_S)	kg/h	11.3×10^6
Rejected seawater mass flow rate (C_W)	kg/h	5.62×10^6
Recycle stream mass flow rate (W_{Re})	kg/h	6.35×10^6
Feed Seawater temperature (T_{sea})	°C	35
Feed seawater salt concentration (C_F)	wt %	5.7
Steam temperature (T_{steam})	°C	97

Based on the above parameters, the seawater desalination process is simulated. Figures 4–8 show the process of the TBT, bottom brine temperature (BBT), and flashing brine temperature of the first three stages (T_{B1} , T_{B2} , T_{B3}), distillate flow rate of the first three stages (W_{D1} , W_{D2} , W_{D3}), and total distillate flow rate (W_{DN}) from a given initial value to steady state during the dynamic simulation process. According to the simulation results, the system reaches a steady state at around 3000 s.

**Figure 4.** Top brine temperature (TBT) dynamic response with time.

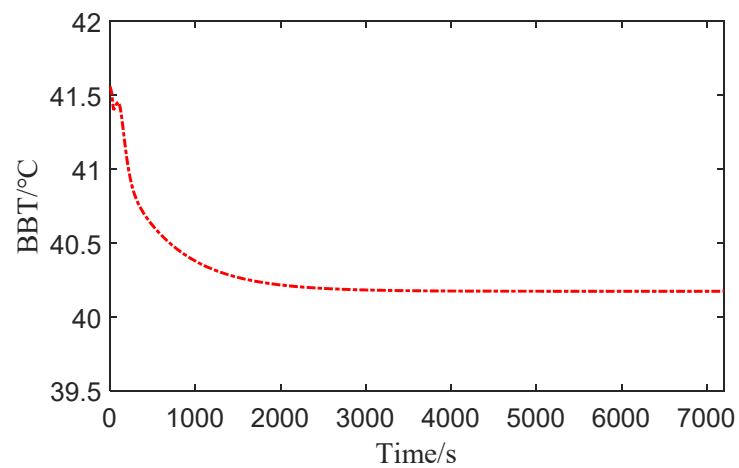


Figure 5. Bottom brine temperature (BBT) dynamic response with time.

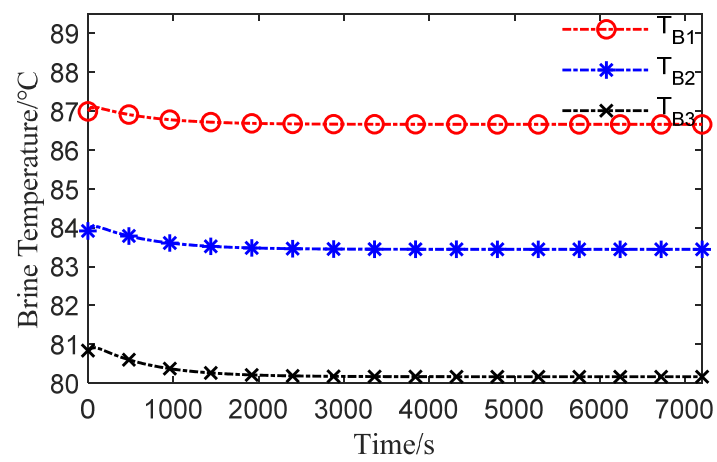


Figure 6. T_{B1} , T_{B2} , T_{B3} dynamic response with time.

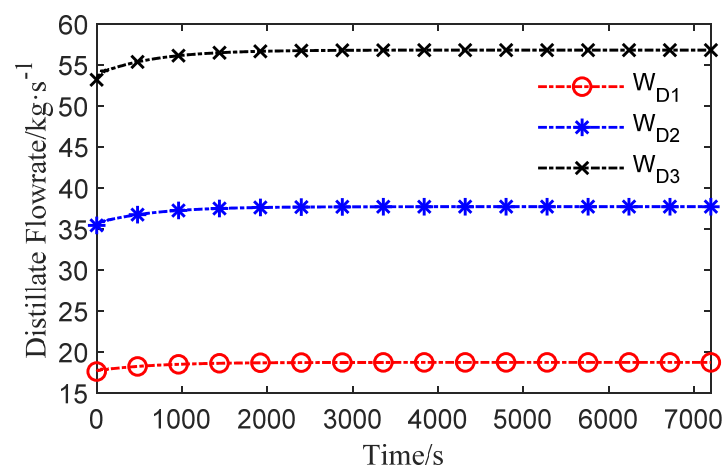


Figure 7. W_{D1} , W_{D2} , W_{D3} dynamic response with time.

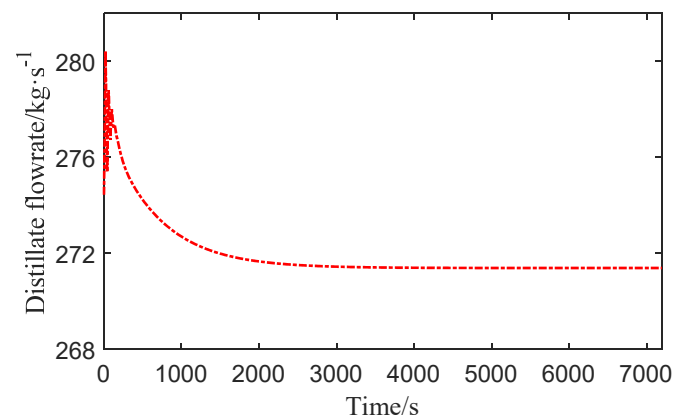


Figure 8. W_{DN} dynamic response with time.

As the system device parameters cannot be completely consistent with the references, there are certain difficulties in proof of the exact same dynamic characteristics. Hence, the steady-state results of the dynamic system are compared with the results of Gao Hanhan et al. [32]. The steady-state model simulation results are shown in the paper of Gao Hanhan et al. [32], and the simulation results are in good agreement with Rosso et al. [31]. The steady-state value of the dynamic model after 3000 s is extracted.

Since the dynamic response of disturbance will drive the multistage flash process from one steady state to another steady state, at that time, the final value of dynamic response should be consistent with the new balanced steady state. Hence, the validation is carried out as follows. Assuming that the level of all stages of flashing brine is 0.457 m, the initial values are calculated based on the results of the steady-state model. Based on the dynamic model established above, the dynamic simulation of the system is carried out under the MATLAB platform.

According to Figures 4–8, the system reaches a steady state around 3000 s. The steady-state value of the system after 3000 s is extracted. Figure 9 shows both the flashing brine temperature after 3000 s during the dynamic process (T_{Bj}) and the flashing brine temperature within the steady-state simulation results (T_{Bj}^0) of Gao Hanhan et al. [32]. Figure 10 shows both the distillate temperature after 3000 s during the dynamic process (T_{Dj}) and the distillate temperature during the steady-state process (T_{Dj}^0). Figure 11 shows the distillate flow rate after 3000 s during the dynamic process (W_{Dj}) and the distillate flow rate during the steady-state process at all stages (W_{Dj}^0). The undisturbed simulation results of the dynamic model established in this paper are consistent with the steady-state simulation results of Gao Hanhan et al. [32].

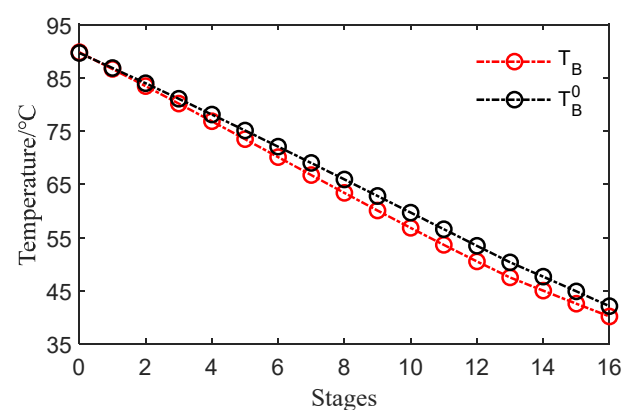


Figure 9. T_{Bj} distribution comparison.

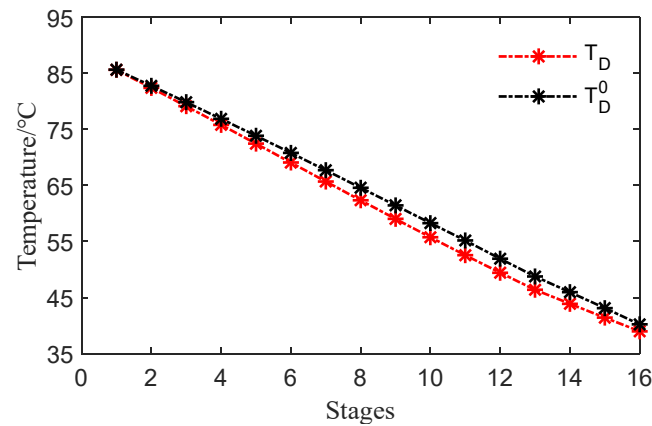


Figure 10. T_{Dj} distribution comparison.

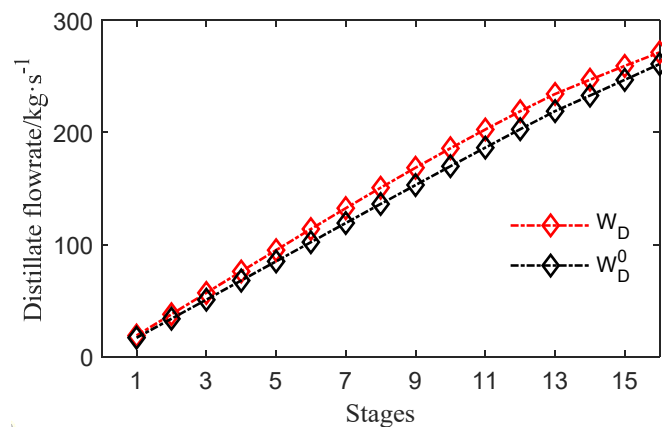


Figure 11. W_{Dj} distribution comparison.

4. Dynamic Simulation and Analysis

In order to study the performance changes of the multistage flash desalination system under different working conditions, based on the dynamic model established above, the influence of T_{sea} , W_{Re} , and T_{steam} on the performance of the system is discussed in this paper.

4.1. Dynamic Response Analysis of Feed Seawater Temperature Change

Seawater temperature is a variable input affected by external disturbances, which will change with the seasons and different times of the day. It is meaningful to analyze the impact of T_{sea} changes on the system. Under the condition that other operating parameters remain unchanged, T_{sea} increases (from 35 to 39 °C) during the simulation process.

As shown in Figure 12, when the system runs normally to 4000 s, a disturbance is caused by the increase of T_{sea} by 300 s; that is, T_{sea} increases from 35 to 39 °C. When the system runs to 4300 s, the disturbance stops and T_{sea} recovers to 35 °C and this lasts until the end of 7200 s.

The dynamic responses of the T_{sea} increase are shown in Figures 13–16. The disturbance time of the T_{sea} increase is 5 min, and the dynamic response time of TBT, BBT, T_{B1} , T_{B2} , T_{B3} , and W_{D1} , W_{D2} , W_{D3} is about 8 min. The results show that the changes of TBT, BBT, and T_{B1} , T_{B2} , T_{B3} are proportional to the change of T_{sea} . BBT is more sensitive to the change in T_{sea} than TBT. However, the change in W_{D1} , W_{D2} , W_{D3} is inversely proportional to the change in T_{sea} , showing a downward trend at first and then an upward trend. The dynamic trends of TBT, BBT, and T_{B1} , T_{B2} , T_{B3} with increasing seawater temperature, are the same as in the paper by Jari et al. [22].

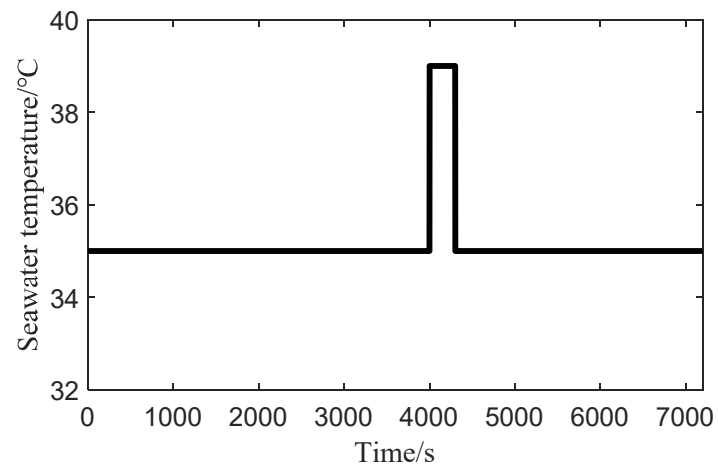


Figure 12. Disturbance of T_{sea} increase.

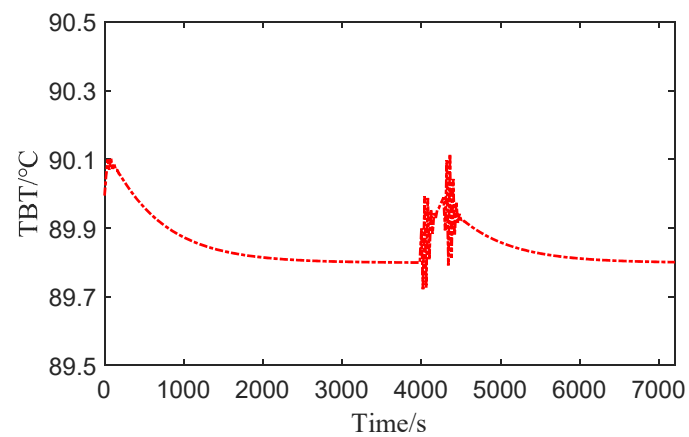


Figure 13. Dynamic of TBT for step increase in T_{sea} .

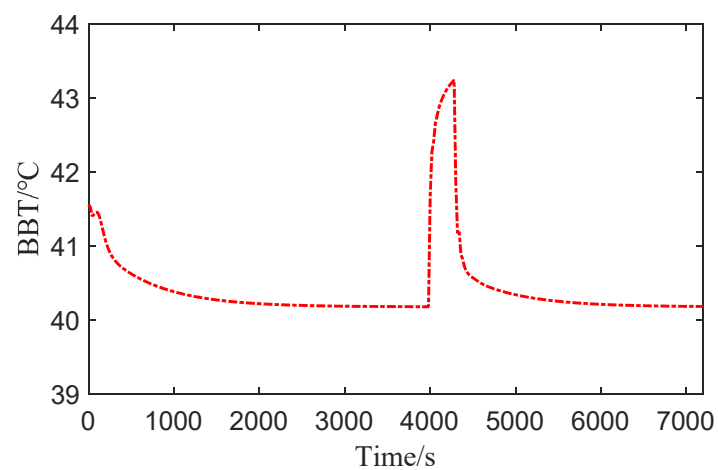


Figure 14. Dynamic of BBT for step increase in T_{sea} .

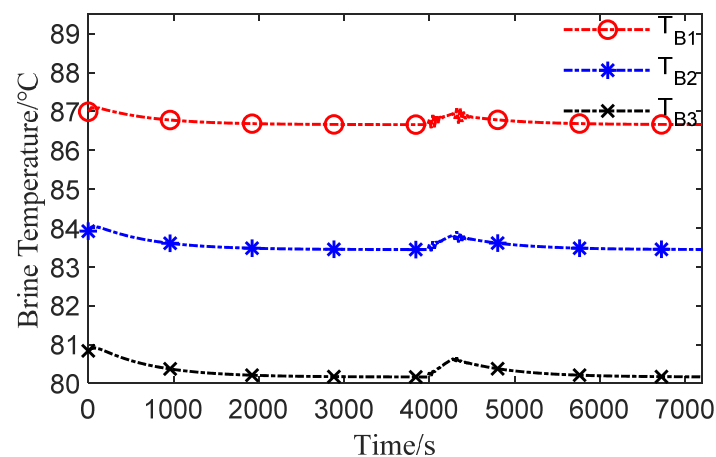


Figure 15. Dynamic of T_{B1} , T_{B2} , T_{B3} for step increase in T_{sea} .

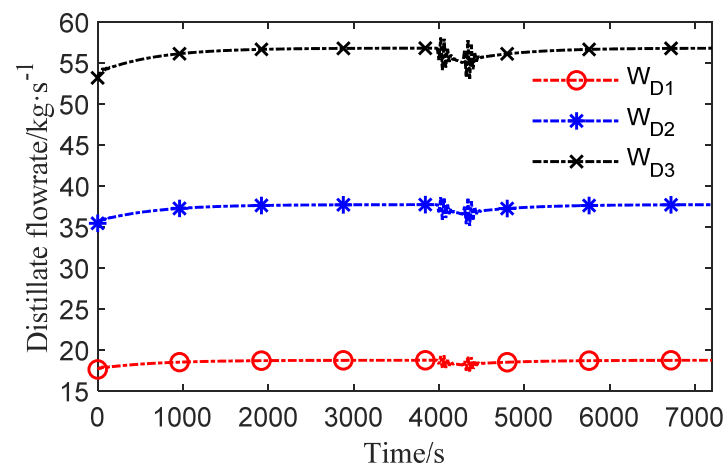


Figure 16. Dynamic of W_{D1} , W_{D2} , W_{D3} for step increase in T_{sea} .

The dynamic responses of TBT, BBT, and T_{B1} , T_{B2} , T_{B3} are shown in Figures 13–15. The figures show that the rise of the above parameters is smaller than that of the disturbance. The increase in T_{sea} reduces the overall temperature drop of the device, indicating a decrease in the heat consumption of the flashing brine in the system. According to the law of conservation of energy, the heat lost by the flashing brine will be converted into the heat absorbed by the flashing steam, resulting in less distillate. Therefore, as shown in Figure 16, when the disturbance occurs, W_{D1} , W_{D2} , W_{D3} will first decrease and then increase.

4.2. Dynamic Response Analysis of Feed Seawater Salt Concentration Change

C_F is one of the important parameters that are susceptible to external influences in the MSF-BR process, and its change will also affect the performance of the entire device. Under the condition that other operating parameters remain unchanged, C_F is increased (from 5.7 to 6.7 wt %) during the simulation process.

As shown in Figure 17, when the system runs normally to 4000 s, a disturbance is caused by the increase of C_F by 300 s; that is, C_F increases from 5.7 to 6.7 wt %. When the system runs to 4300 s, the disturbance stops and C_F recovers to 5.7 wt % and this lasts until the end of 7200 s.

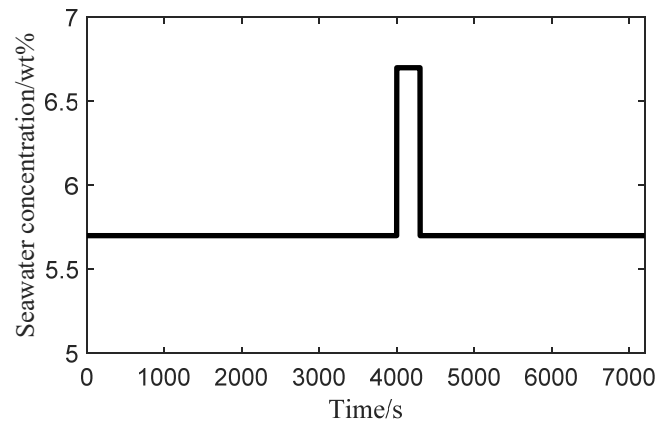


Figure 17. Disturbance of the decrease in C_F .

The dynamic responses of the increase in C_F are shown in Figures 18–21. The disturbance time of the C_F increase is 5 min, and the dynamic response time of TBT, BBT, T_{B1} , T_{B2} , T_{B3} , and W_{D1} , W_{D2} , W_{D3} is about 6 min.

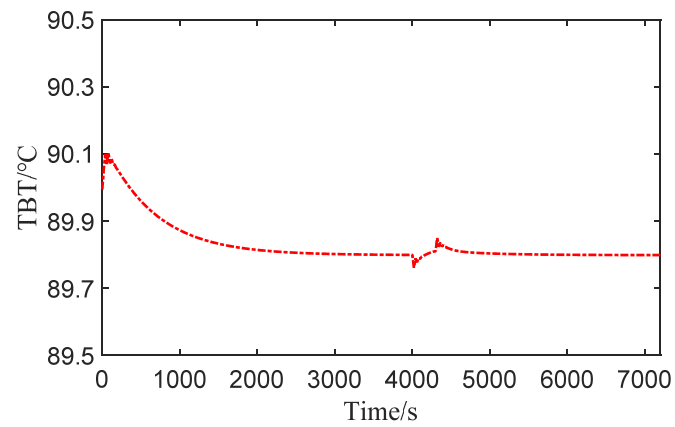


Figure 18. Dynamic of TBT for step increase in C_F .

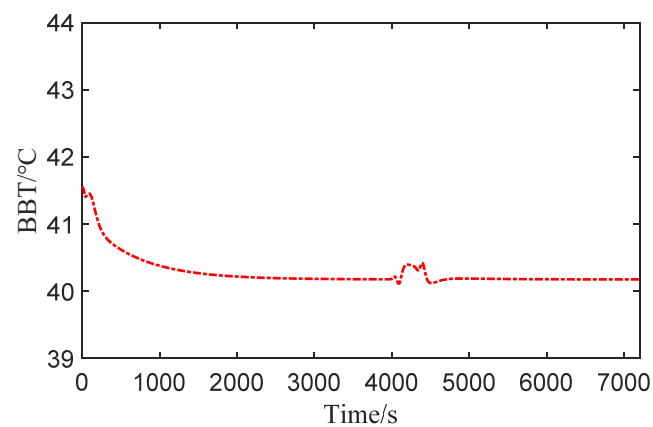


Figure 19. Dynamic of BBT for step increase in C_F .

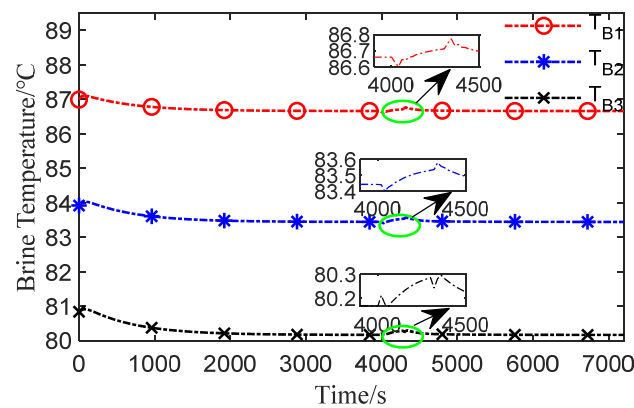


Figure 20. Dynamic of T_{B1} , T_{B2} , T_{B3} for step increase in C_F .

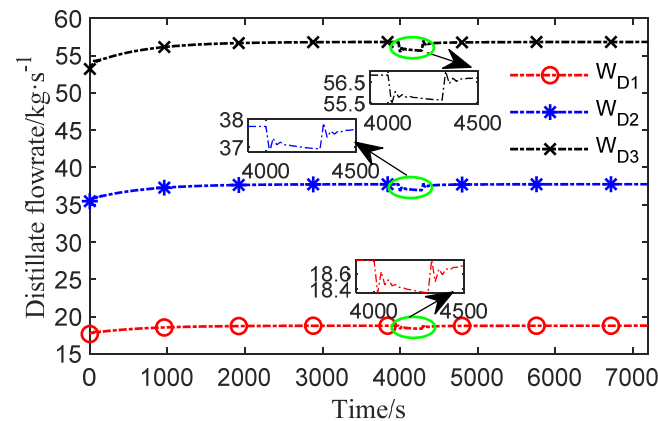


Figure 21. Dynamic of W_{D1} , W_{D2} , W_{D3} for step increase in C_F .

C_F affects the related physical parameters of the system, thus affecting system performance. It can be seen from Equation (32) that the change in C_F will lead to the change in the BPE_j value, which will affect the T_{Bj} of the flash chambers. The change in T_{Bj} will affect the flash temperature drop of the whole system and then affect distillate production.

Therefore, as shown in Figures 18–20, the first increase and then decrease of the feed seawater salt concentration made TBT and T_{B1} , T_{B2} , T_{B3} decrease and then increase, with little effect. As shown in Figure 19, the variation trend of BBT is consistent with the trend of the disturbance of C_F , with little influence.

As shown in Figure 21, due to the first TBT decrease and then increase, the overall flash temperature drop of the system will decrease and then increase accordingly. According to the conservation of energy, W_{D1} , W_{D2} , W_{D3} also decreases first and then increases.

4.3. Dynamic Response Analysis of Recycle Stream Mass Flow Rate Change

W_{Re} is one of the important parameters in the MSF-BR process, and it is also one of the adjustable parameters. The study of the influence of W_{Re} on dynamic performance can provide a deeper understanding of the dynamic characteristics of the system and provide a path to dynamic optimization of the system in the future. Under the condition that other operating parameters remain unchanged, W_{Re} is increased (from 6.05×10^6 to 6.35×10^6 kg/h) during the simulation process.

As shown in Figure 22, when the system runs normally to 4000 s, a disturbance is caused by the increase of W_{Re} by 300 s; that is, W_{Re} increases from 6.05×10^6 to 6.35×10^6 kg/h. When the system runs to 4300 s, the disturbance stops and W_{Re} recovers to 6.05×10^6 kg/h and this lasts until the end of 7200 s.

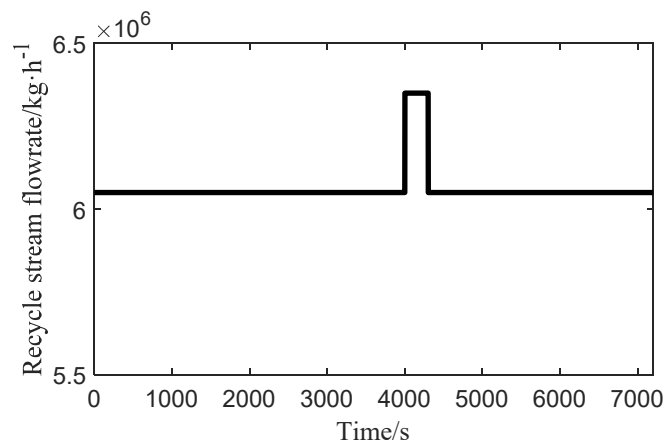


Figure 22. Disturbance of the W_{Re} increase.

The dynamic responses of the W_{Re} increase are shown in Figures 23–26. The disturbance time of the W_{Re} increase is 5 min, and the dynamic response time of TBT, BBT, T_{B1} , T_{B2} , T_{B3} , and W_{D1} , W_{D2} , W_{D3} is about 6 min. The range of fluctuation is small, and the steady-state value before and after the fluctuation does not change much.

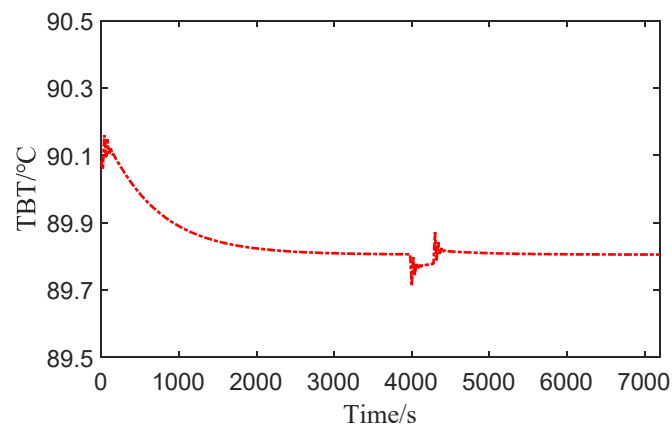


Figure 23. Dynamic of TBT for step increase in W_{Re} .

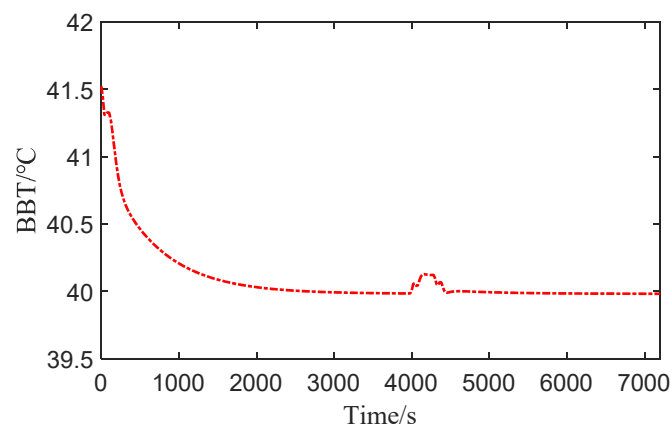


Figure 24. Dynamic of BBT for step increase in W_{Re} .

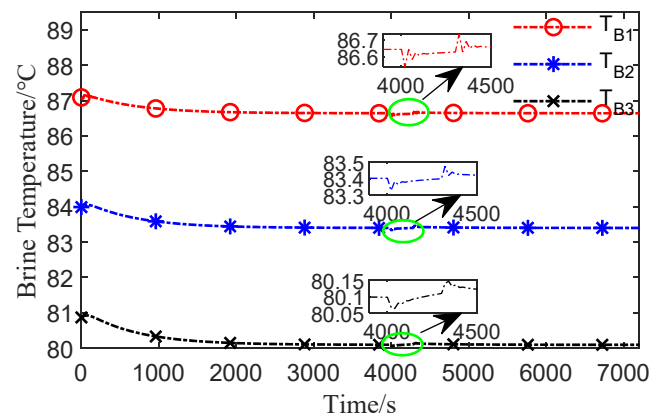


Figure 25. Dynamic of T_{B1} , T_{B2} , T_{B3} for step increase in W_{Re} .

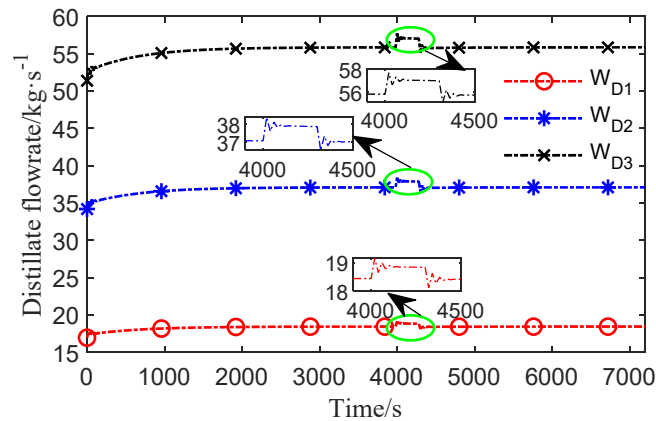


Figure 26. Dynamic of W_{D1} , W_{D2} , W_{D3} for step increase in W_{Re} .

W_{Re} is mixed with the make-up brine mass flow rate (W_m) from the heat rejection section and enters the condenser tubes of the heat recovery section for preheating. After mixing, the cooling brine mass flow rate to the recovery section (W_R) will then enter the brine heater for heating. Obviously, the increase in W_{Re} will reduce the temperature of the cooling brine to the brine heater (T_{F0}). As shown in Figures 23–25, the first increase and then decrease in W_{Re} will lead to the decrease and then increase of T_{B1} , T_{B2} , T_{B3} and TBT.

The increase in W_{Re} has little effect on BBT. For the later flash chamber of the system, the increase in W_{Re} is equivalent to the increase in W_{Bj} in the flash chamber. Under the effect of the fixed interstage pressure difference of the system, T_{Bj} cannot drop to the previous ideal temperature but may increase instead. As shown in Figure 24, the first increase and then decrease of W_{Re} will cause BBT to decrease first and then increase.

As shown in Figure 26, because W_{Re} first decreases and then increases, the overall seawater of the device increases first and then decreases. Hence, W_{D1} , W_{D2} , W_{D3} increases first and then decreases.

4.4. Dynamic Response Analysis of Steam Temperature Change

The temperature of steam directly affects the size of TBT and then affects the performance of the whole device. Under the condition that other operating parameters remain unchanged, T_{steam} increases (from 97 to 99 °C) during the simulation process.

As shown in Figure 27, when the system runs normally to 4000 s, a disturbance is caused by the increase of T_{steam} ; that is, T_{steam} increases from 97 to 99 °C and this lasts until the end of 7200 s.

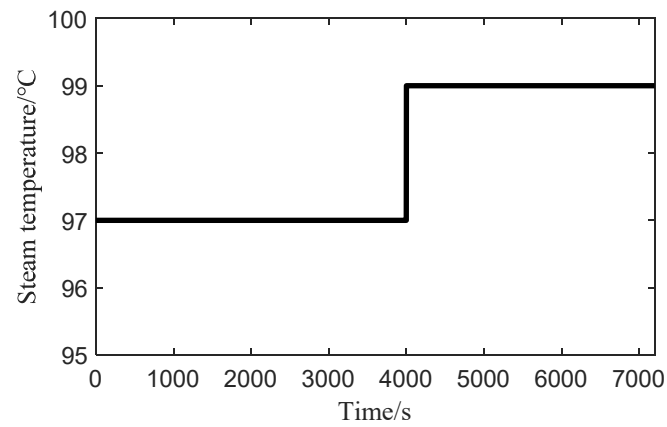


Figure 27. Disturbance of the T_{steam} increase.

The dynamic responses of the T_{steam} increase are shown in Figures 28–31. The dynamic response time of TBT, BBT, T_{B1} , T_{B2} , T_{B3} and W_{D1} , W_{D2} , W_{D3} is about 2 min.

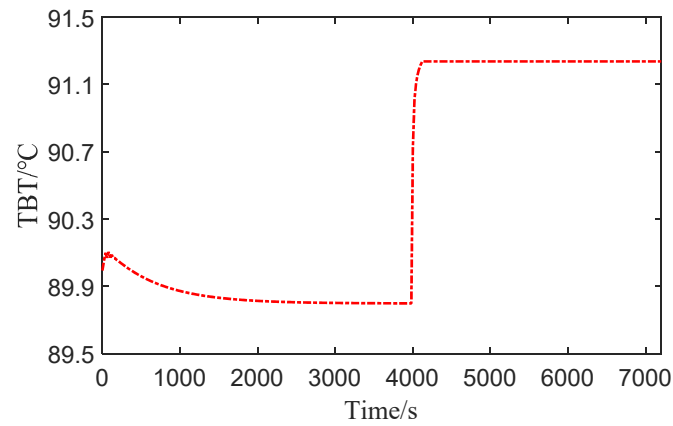


Figure 28. Dynamic of TBT for step increase in T_{steam} .

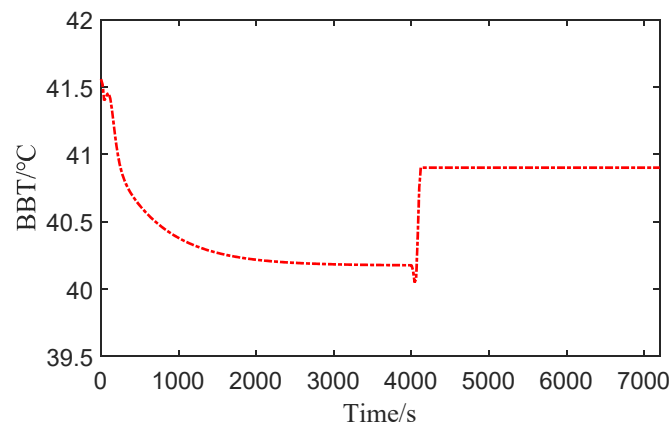


Figure 29. Dynamic of BBT for step increase in T_{steam} .

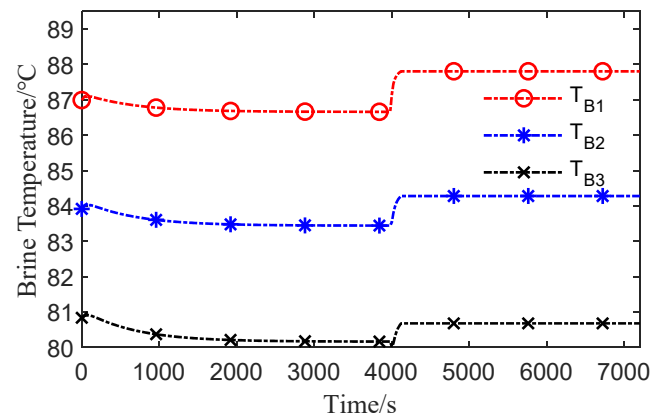


Figure 30. Dynamic of T_{B1} , T_{B2} , T_{B3} for step increase in T_{steam} .

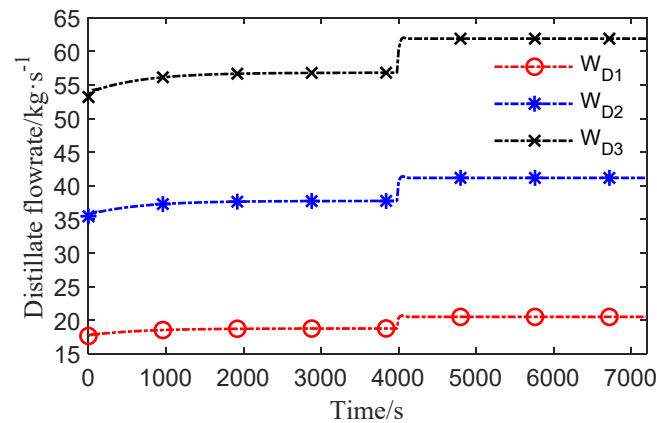


Figure 31. Dynamic of W_{D1} , W_{D2} , W_{D3} for step increase in T_{steam} .

Cooling seawater (W_{F0}) enters the brine heater from the outlet of the condenser tubes of the first-stage flash chamber, and W_{steam} releases latent heat to heat the brine in the device. At the outlet of the brine heater, W_{B0} enters the brine pool of the first-stage flash chamber at TBT to start the flashing. T_{steam} directly affects TBT and T_{B1} , T_{B2} , T_{B3} . As shown in Figures 28–30, with the increase in T_{steam} , both TBT and T_{B1} , T_{B2} , T_{B3} increase, which has a great influence. Compared with TBT, the increase in T_{steam} has little influence on BBT.

Due to the increase of TBT, the flash temperature drop of the system will increase. Hence, as shown in Figure 31, under the condition that other operating parameters remain unchanged, W_{D1} , W_{D2} , W_{D3} will increase.

5. Conclusions

Multistage flash is one of the most widely used desalination methods, and its dynamic performance is very important for optimal operation, design, maintenance, and fault diagnosis. In this paper, the dynamic modeling and simulation of the multistage flash process were studied for the purpose of easy implementation and real-time operation. Based on more detailed consideration, a whole-process dynamic model, including a brine heat exchanger, a flashing stage room, mixed and split modulates, and physical parameter modulate, was established. For quick simulation, the dynamic equations were discretized and put together with physical equations through a simultaneous strategy and solved using the Interior Point solver, with sparsity treatment under the MATLAB platform. Then, the validation and solving efficiencies were verified by a multistage flash desalination system with 16 stages. In addition, the dynamic response for different key parameters such as feed seawater temperature, feed seawater concentration, recycle stream mass flow rate, and steam temperature were simulated and analyzed. The simulation results can also provide

ideas for the combination of the variable changes that make the system operate with more stability. For example, the distillate flow rate decreases with the increase of feedwater concentration but increases with the steam temperature; therefore, it could be reasonable to think that increasing the steam temperature when the feedwater concentration increases is a kind of control strategy to maintain the levels of distillate in the plant. The states of each stage and the key permeance curve of TBT and BBT were also obtained and analyzed under dynamic change. The presented dynamic model and its treatment can provide a better understanding and analysis for real-time optimal operation and control of the MSF system to achieve lower operational cost and more stable freshwater quality.

Author Contributions: Q.-Y.H. performed the simulations and analyzed the data, A.-P.J. designed the process scheme of the paper, Q.-Y.H., H.-Y.Z., and J.W. wrote the paper and reviewed it. Y.-D.X. and L.H. checked the results of the whole manuscript. All authors have read and agreed to the published version of the manuscript.

Funding: This research was funded by the Natural Science Foundation of Zhejiang (grant No. LY20F030010), the National Natural Science Foundation of China (grant No. 61973102), and the Foundation of Zhejiang Provincial Education Department of China (grant No. Y202044268).

Institutional Review Board Statement: Not applicable.

Informed Consent Statement: Not applicable.

Data Availability Statement: The data presented in this study are available on request from the corresponding author. The data are not publicly available due to the privacy.

Conflicts of Interest: The authors declare no conflict of interest.

Abbreviations

In order to better understand the mathematical model of MSF seawater desalination, a symbol description list is added here.

A_H	Heat transfer area of the brine heater, m^2
A_j	Heat transfer area of stage j, m^2
BPE_j	Boiling point elevation of stage j
C_{B0}	Salt concentration in the flashing leaving the brine heater, wt %
C_{Bj}	Salt concentration in the flashing brine leaving stage j, wt %
C_{F0}	Salt concentration of flashing seawater leaving brine heater, wt %
C_{Fj}	Salt concentration of flashing seawater leaving stage j, wt %
C_m	Salt concentration in make-up water, wt %
C_R	Salt concentration in the cooling brine to the recovery section, wt %
C_{Re}	Recycle brine concentration, wt %
C_W	Rejected seawater mass flow rate, $kg \cdot h^{-1}$
CP_{Bj}	Heat capacity of brine leaving stage j, $kcal \cdot (kg \cdot ^\circ C)^{-1}$
CP_{Dj}	Heat capacity of distillate leaving stage j, $kcal \cdot (kg \cdot ^\circ C)^{-1}$
CP_{Fj}	Heat capacity of flashing seawater leaving stage j, $kcal \cdot (kg \cdot ^\circ C)^{-1}$
CP_{Vj}	Heat capacity of flashing steam leaving stage j, $kcal \cdot (kg \cdot ^\circ C)^{-1}$
CP_{RH}	Heat capacity of cooling brine leaving brine heater, $kcal \cdot (kg \cdot ^\circ C)^{-1}$
D_H^i	Internal diameter of condenser tube, m
D_H^o	External diameter of condenser tube, m
D_j^i	Internal diameter of condenser tube at stage j, m
D_j^o	External diameter of condenser tube at stage j, m
F_{Dj}	Steam condensation at stage j, $kg \cdot h^{-1}$
f_{BH}	Brine heater fouling factor, $h \cdot m^2 \cdot ^\circ C \cdot kcal^{-1}$
f_j	Fouling factor at stage j, $h \cdot m^2 \cdot ^\circ C \cdot kcal^{-1}$
H_j	Height of condenser tube at stage j, m
h_{Bj}	Specific enthalpy of flashing brine at stage j, $kcal \cdot kg^{-1}$

h_{B0}	Specific enthalpy of flashing brine at brine heater, $\text{kcal}\cdot\text{kg}^{-1}$
h_{Dj}	Specific enthalpy of distillate at stage j, $\text{kcal}\cdot\text{kg}^{-1}$
h_{VBj}	Specific enthalpy of steam at stage j, $\text{kcal}\cdot\text{kg}^{-1}$
h_{Fj}	Specific enthalpy of flashing seawater at stage j, $\text{kcal}\cdot\text{kg}^{-1}$
h_{FDj}	Specific enthalpy of condensation at stage j, $\text{kcal}\cdot\text{kg}^{-1}$
h_m	Specific enthalpy of make-up brine, $\text{kcal}\cdot\text{kg}^{-1}$
h_R	Specific enthalpy of stream to recovery section, $\text{kcal}\cdot\text{kg}^{-1}$
h_{Re}	Specific enthalpy of recycled brine, $\text{kcal}\cdot\text{kg}^{-1}$
h_S	Specific enthalpy of recycled brine at rejection stage, $\text{kcal}\cdot\text{kg}^{-1}$
h_{Vj}	Specific enthalpy of steam at stage j, $\text{kcal}\cdot\text{kg}^{-1}$
h_{WF}	Specific enthalpy of brine at the entrance of rejection section, $\text{kcal}\cdot\text{kg}^{-1}$
h_{WS}	Specific enthalpy of feed seawater, $\text{kcal}\cdot\text{kg}^{-1}$
L_H	Length of brine heater condenser tube, m
L_j	Length of condenser tube at stage j, m
M_{Bj}	Flashing brine holdup at stage j, kg
M_{B0}	Flashing brine holdup at brine heater, kg
M_{Dj}	Distillate holdup at stage j, kg
M_{Vj}	Flashing steam holdup at stage j, kg
M_{Fj}	Flashing seawater holdup at stage j, kg
N	Total number of stages, $N = N_R + N_J$
$NETD$	Nonequilibrium allowance, $^{\circ}\text{C}$
N_J	Number of stages in the heat rejection section
N_R	Number of stages in the heat recovery section
N_{TUBE}	Number of condenser tubes
N_f	Degree of freedom
N_v	Number of variables
N_e	Number of independent differential and algebraic equations
S	Reject recycled mass flow rate, $\text{kg}\cdot\text{h}^{-1}$
T_{Bj}	Temperature of flashing brine leaving stage j, $^{\circ}\text{C}$
T_{B0}	Temperature of flashing brine leaving the brine heater, $^{\circ}\text{C}$
T_{Dj}	Temperature of distillate leaving stage j, $^{\circ}\text{C}$
T_{Fj}	Temperature of cooling brine leaving stage j, $^{\circ}\text{C}$
T_{F0}	Temperature of cooling brine to brine heater, $^{\circ}\text{C}$
TL_j	Temperature loss due to demister and condenser, $^{\circ}\text{C}$
T_{Vj}	Temperature of flashed vapor at stage j, $^{\circ}\text{C}$
T_{sea}	Seawater temperature, $^{\circ}\text{C}$
T_{steam}	Steam temperature, $^{\circ}\text{C}$
U_H	Overall heat transfer coefficient at the brine heater, $\text{kcal}\cdot(\text{m}^2\cdot\text{h}\cdot^{\circ}\text{C})^{-1}$
U_j	Overall heat transfer coefficient at stage j, $\text{kcal}\cdot(\text{m}^2\cdot\text{h}\cdot^{\circ}\text{C})^{-1}$
V_{Bj}	Evaporation capacity of brine at stage j, $\text{kg}\cdot\text{h}^{-1}$
V_{TUBE}	Volume of condenser tube, m^3
W_{B0}	Flashing brine mass flow rate leaving brine heater, $\text{kg}\cdot\text{h}^{-1}$
W_{BD}	Blowdown mass flow rate, $\text{kg}\cdot\text{h}^{-1}$
W_{Bj}	Flashing Brine mass flow rate leaving stage j, $\text{kg}\cdot\text{h}^{-1}$
W_{BN}	Flashing Brine mass flow rate leaving stage N, $\text{kg}\cdot\text{h}^{-1}$
W_{Dj}	Distillate mass flow rate leaving stage j, $\text{kg}\cdot\text{h}^{-1}$
W_{DN}	Distillate mass flow rate leaving stage N, $\text{kg}\cdot\text{h}^{-1}$
W_F	Flashing seawater mass flow rate to rejection section, $\text{kg}\cdot\text{h}^{-1}$
W_{Fj}	Flashing seawater mass flow rate leaving stage j, $\text{kg}\cdot\text{h}^{-1}$
w_j	Width of condenser tube at stage j, m
W_m	Make-up brine mass flow rate, $\text{kg}\cdot\text{h}^{-1}$
W_R	Cooling brine mass flow rate to recovery section, $\text{kg}\cdot\text{h}^{-1}$
W_r	Mass flow rate to the reject seawater splitter, $\text{kg}\cdot\text{h}^{-1}$
W_{Re}	Recycle stream mass flow rate, $\text{kg}\cdot\text{h}^{-1}$
W_S	Seawater mass flow rate, $\text{kg}\cdot\text{h}^{-1}$
W_{steam}	Steam mass flow rate, $\text{kg}\cdot\text{h}^{-1}$

ρ_{Bj}	Density of flashing brine at stage j, $\text{kg}\cdot\text{m}^{-3}$
ρ_{Dj}	Density of distillate at stage j, $\text{kg}\cdot\text{m}^{-3}$
ρ_{Vj}	Density of steam at stage j, $\text{kg}\cdot\text{m}^{-3}$
ΔTL_j	Temperature difference loss, $^{\circ}\text{C}$

References

- Bourouis, M.; Pibouleau, L.; Floquet, P.; Domenech, S.; Al-Gobaisi, D.M.K. Simulation and data validation in multistage flash desalination plants. *Desalination* **1998**, *115*, 1–14. [[CrossRef](#)]
- Zhang, B.-Z. Multi-stage flash seawater desalination technology. *CFHI Technol.* **2008**, *4*, 48–49.
- Qiu, M.-Y. Analysis of seawater desalination technology in China. *China Environ. Prot. Ind.* **2008**, *4*, 58–60.
- Zhao, Z.-H.; Yuan, Y.-C.; Chen, Y. Analysis of multi-stage flash seawater desalination technology. *Sci. Mosaic* **2017**, *8*, 46–49.
- Xie, L.-X.; Li, P.-L.; Wang, S.-C. Current status of seawater desalination technology and review of various desalination methods. *Chem. Ind. Eng. Prog.* **2003**, *10*, 55–58.
- Jin, Y.-X. Water resources crisis under global warming. *Ecol. Econ.* **2020**, *36*, 5–8.
- Helal, A.M. Once-through and brine recirculation MSF designs—A comparative study. *Desalination* **2004**, *171*, 33–60. [[CrossRef](#)]
- Ettouney, H.; Eldessouky, H.; Aljuwayhel, F. Performance of the once-through multistage flash desalination process. *Proc. Inst. Mech. Eng. Part A J. Power Energy* **2002**, *216*, 229–241. [[CrossRef](#)]
- Aly, N.H.; Marwan, M.A. Dynamic behavior of MSF desalination plants. *Desalination* **1995**, *101*, 287–293. [[CrossRef](#)]
- Glueck, A.R.; Bradshaw, R.W. A mathematical model for a multistage flash distillation plant. *Dubrov. Yugosl.* **1970**, *1*, 95–108.
- Ulrich. *Dynamic Behaviors of MSF Plants for Seawater Desalination*; University of Hannover: Hannover, Germany, 1977; pp. 126–134.
- Rimawi, M.A.; Ettouney, H.M.; Aly, G.S. Transient model of Multistage flash desalination. *Desalination* **1989**, *74*, 327–338. [[CrossRef](#)]
- Asghar, H.; Ali, H.; Al-Gobaisi, D.M.K.; Al-Radif, A.; Woldai, A.; Sommariva, C. Modelling, simulation, optimization and control of multistage flashing (MSF) desalination plants Part I: Modelling and simulation. *Desalination* **1993**, *92*, 21–41.
- Husain, A.; Woldai, A.; Al-Radif, A.; Kesou, A.; Borsani, R.; Sultan, H.; Deshpandey, P.B. Modelling and simulation of a multistage flash (MSF) desalination plant. *Desalination* **1994**, *97*, 555–586. [[CrossRef](#)]
- Rizzuti, L.; Ettouney, H.M.; Cipollina, A. Dynamic modeling tools for solar powered desalination process during transient operations. In *Solar Desalination for the 21st Century*; Springer: Dordrecht, The Netherlands, 2007; pp. 43–67.
- Mazzotti, M.; Rosso, M.; Beltramini, A.; Morbidelli, M. Dynamic modeling of multistage flash desalination plants. *Desalination* **2000**, *127*, 207–218. [[CrossRef](#)]
- Alatiqi, I.; Ettouney, H.; El-Dessouky, H.; Al-Hajri, K. Measurements of dynamic behavior of a multistage flash water desalination system. *Desalination* **2004**, *160*, 233–251. [[CrossRef](#)]
- Hala, A.; Andrea, C.; Hisham, E.; David, B. Simulation of stability and dynamics of multistage flash desalination. *Desalination* **2011**, *281*, 404–412.
- Alsadaie, S.M.; Mujtaba, I.M. Generic Model Control (GMC) in Multistage Flash (MSF) Desalination. *J. Process. Control.* **2016**, *44*, 92–105. [[CrossRef](#)]
- Alsadaie, S.M.; Mujtaba, I.M. Modelling and simulation of MSF desalination plant: The effect of venting system design for non-condensable gases. *Chem. Eng. Trans.* **2014**, *39*, 1615–1620.
- Alsadaie, S.M.; Mujtaba, I.M. Dynamic modelling of heat exchanger fouling in multistage flash (MSF) desalination. *Desalination* **2017**, *409*, 47–65. [[CrossRef](#)]
- Jari, L.; Timo, K.; Ville, A. Modelling and dynamic simulation of a large MSF plant using local phase equilibrium and simultaneous mass, momentum, and energy solver. *Comput. Chem. Eng.* **2017**, *97*, 242–258.
- Al-Fulaij, H.F. Dynamic Modeling of Multi Stage Flash (MSF) Desalination Plant. Ph.D. Thesis, University College London, London, UK, 2011.
- Helal, A.M.; El-Nashar, A.M.; Al-Katheeri, E.; Al-Malek, S.A. Optimal design of hybrid RO/MSF desalination plants Part I: Modeling and algorithms. *Desalination* **2003**, *154*, 43–66. [[CrossRef](#)]
- Helal, A.M.; El-Nashar, A.M.; Al-Katheeri, E.; Al-Malek, S.A. Optimal design of hybrid RO/MSF desalination plants part II: Results and discussion. *Desalination* **2004**, *160*, 13–27. [[CrossRef](#)]
- Helal, A.M.; El-Nashar, A.M.; Al-Katheeri, E.; Al-Malek, S.A. Optimal design of hybrid RO/MSF desalination plants part III: Sensitivity analysis. *Desalination* **2004**, *169*, 43–60. [[CrossRef](#)]
- El-Dessouky, H.T.; Ettouney, H.M. *Fundamentals of Salt Water Desalination*, 1st ed.; Elsevier Science B.V.: Amsterdam, The Netherlands, 2002; pp. 668–670.
- Woldai, A. Operation and control of Multi-Stage flash desalination plants. In *Multi-Stage Flash Desalination*; Ganti, P.R., Andrew, P.S., Eds.; CRC Press: Boca Raton, FL, USA, 2007; Volume 2, pp. 15–35.
- Helal, A.M.; Medani, M.S.; Soliman, M.A. A tridiagonal matrix model for multistage flash desalination plants. *Comput. Chem. Eng.* **1986**, *10*, 327–342. [[CrossRef](#)]
- Al-thalry, H. Single degree of freedom analysis method for steel beams under blast pressure using nonlinear resistance function with strain rate effects. *J. Univ. Babylon Pure Appl. Sci.* **2016**, *24*, 298–313.

-
31. Rosso, M.; Beltramini, A.; Mazzotti, M.; Morbidelli, M. Modeling multistage flash desalination plants. *Desalination* **1997**, *108*, 365–374. [[CrossRef](#)]
 32. Gao, H.-H.; Jiang, A.-P.; Huang, Q.-Y.; Xia, Y.-D.; Gao, F.-R.; Wang, J. Mode-Based Analysis and Optimal Operation of MSF Desalination System. *Processes* **2020**, *8*, 794. [[CrossRef](#)]